This article was downloaded by: [Wuhan University]
On: 07 February 2015, At: 19:10
Publisher: Taylor & Francis
Informa Ltd Registered in England and Wales Registered Number: 1072954 Registered office: Mortimer House, 37-41 Mortimer Street, London W1T 3JH, UK

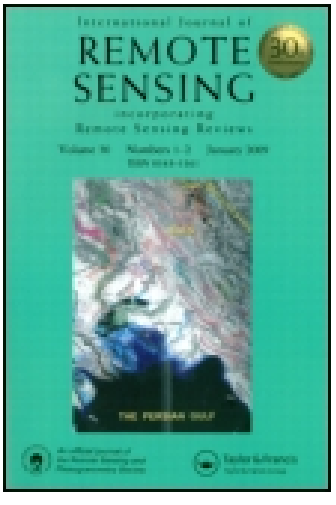

International Journal of Remote Sensing

Publication details, including instructions for authors and subscription information:
http://www.tandfonline.com/loi/tres20

Unsupervised remote sensing image classification using an artificial immune network

Yanfei Zhong [a] , Liangpei Zhang [a] & Wei Gong [a]

[a] State Key Laboratory of Information Engineering in Surveying, Mapping, and Remote Sensing , Wuhan University , Hubei, 430072, PR China

Published online: 11 Aug 2011.

To cite this article: Yanfei Zhong , Liangpei Zhang & Wei Gong (2011) Unsupervised remote sensing image classification using an artificial immune network, International Journal of Remote Sensing, 32:19, 5461-5483, DOI: 10.1080/01431161.2010.502155

To link to this article: http://dx.doi.org/10.1080/01431161.2010.502155

PLEASE SCROLL DOWN FOR ARTICLE

Taylor & Francis makes every effort to ensure the accuracy of all the information (the "Content") contained in the publications on our platform. However, Taylor & Francis, our agents, and our licensors make no representations or warranties whatsoever as to the accuracy, completeness, or suitability for any purpose of the Content. Any opinions and views expressed in this publication are the opinions and views of the authors, and are not the views of or endorsed by Taylor & Francis. The accuracy of the Content should not be relied upon and should be independently verified with primary sources of information. Taylor and Francis shall not be liable for any losses, actions, claims, proceedings, demands, costs, expenses, damages, and other liabilities whatsoever or howsoever caused arising directly or indirectly in connection with, in relation to or arising out of the use of the Content.

This article may be used for research, teaching, and private study purposes. Any substantial or systematic reproduction, redistribution, reselling, loan, sub-licensing, systematic supply, or distribution in any form to anyone is expressly forbidden. Terms & Conditions of access and use can be found at http://www.tandfonline.com/page/terms-and-conditions

International Journal of Remote Sensing
Vol. 32, No. 19, 10 October 2011, 5461–5483

Taylor & Francis
Taylor & Francis Group

Unsupervised remote sensing image classification using an artificial immune network

YANFEI ZHONG, LIANGPEI ZHANG* and WEI GONG
State Key Laboratory of Information Engineering in Surveying, Mapping, and Remote Sensing, Wuhan University, Hubei 430072, PR China

(*Received 16 February 2008; in final form 28 September 2009*)

Downloaded by [Wuhan University] at 19:10 07 February 2015

In this article, the artificial immune network (aiNet) model, a computational intelligent approach based on artificial immune networks (AINs), is applied to remote sensing image processing to improve its intelligence. aiNet has been utilized for clustering, optimization, and data analysis. Nevertheless, due to the inherent complexity of the aiNet algorithm and the large volume of data in remote sensing imagery, the application of aiNet to remote sensing image classification has been rather limited. This article presents an unsupervised artificial immune network for remote sensing image classification (RSUAIN) based on aiNet. The proposed method can adaptively obtain some user-defined parameters, such as clone rate and mutation rate, and evolve the memorial immune network by immune operators and biological properties, such as clone, mutation and memory operators, using the remote sensing image for the task of remote sensing image clustering. Three experiments with different types of images were performed to evaluate the performance of the proposed algorithm and to compare it with other traditional unsupervised classification algorithms, for example, *k*-means, ISODATA (Iterative Self-organizing Data Anaysis Techniques Algorithm) and fuzzy *k*-means. RSUAIN was observed to outperform the traditional algorithms in the three experiments and hence potentially provides an effective option for unsupervised remote sensing image classification.

1. Introduction

Artificial immune networks (AINs), derived from immune network theory, are important and effective models of artificial immune systems (AISs) and have been successfully applied to pattern recognition, parallel distributed processing and data analysis (Dasgupta 1999, De Castro and Timmis 2002a). In particular, a novel immune network model, namely the artificial immune network (aiNet), has been shown to be effective for data clustering (De Castro and Von Zuben 2000, 2001, De Castro and Timmis 2002b), multimodal function optimization (De Castro and Timmis 2002c, Timmis and Edmonds 2004) and multimodal electromagnetic problems (Campelo *et al.* 2006). However, only a few applications of AINs have been reported in the field of remote sensing (Zhang *et al.* 2007, Zhong *et al.* 2007, Pal 2008). The slow adaption of AINs may be attributed to the high computational costs arising from the original algorithm with the large volume of remote sensing data, which render it less attractive

*Corresponding author. Email: zlp62@lmars.whu.edu.cn

International Journal of Remote Sensing
ISSN 0143-1161 print/ISSN 1366-5901 online © 2011 Taylor & Francis
http://www.tandf.co.uk/journals
DOI: 10.1080/01431161.2010.502155

for remote sensing image classification. For example, aiNet has been applied to the clustering of standard datasets (iris data, wine data, etc.) (Liu and Xu 2006), which were usually far smaller than remote sensing images. The large number of user-defined parameters is another problem. To overcome these shortcomings and benefit from the advantages of aiNet for clustering, this article exploits an artificial immune network to perform unsupervised remote sensing image classification.

Compared to supervised classification, unsupervised remote sensing image classification normally requires only a minimal amount of initial input from the analyst because clustering does not normally require training data (Jensen 2005). Traditional unsupervised classification algorithms, such as *k*-means (Duda *et al*. 2001) and the Iterative Self-organizing Data Anaysis Techniques Algorithm (ISODATA) (Hall and Ball 1965), use iterative calculations to find an optimum set of decision boundaries for clustering. The ISODATA is a more sophisticated version of *k*-means, which allows classes to be split and merged. For the above hard partitional clustering, each pattern only belongs to one cluster. However, a pixel may also be allowed to belong to all clusters with a degree of membership using the fuzzy clustering algorithms, e.g. fuzzy *k*-means (Campbell 2000, Jensen 2005). In addition to the aforementioned algorithms, Bayesian classifiers (Storvik *et al.* 2005), Markov random field (Yamazaki and Gingras 1999), Kohonen's self-organizing maps (SOM) (Bagan *et al.* 2005) and genetic algorithms (GA) (Bandyopadhyay *et al.* 2007) have also been employed to obtain better unsupervised classification results.

This article describes the remote sensing unsupervised artificial immune network (RSUAIN), which utilizes the advantages of aiNet and is designed to overcome the shortcomings of the original aiNet for the unsupervised remote sensing image classification approach. Compared with the conventional aiNet, the proposed algorithm decreases the number of user-defined parameters required by the adaptive method in the process of execution and is more suitable for classification of remote sensing imagery. The proposed algorithm has been tested and compared with other algorithms using various remote sensing images. Experimental results suggest that the algorithm can achieve high classification accuracy, thus providing an effective option for unsupervised remote sensing image classification.

Downloaded by [Wuhan University] at 19:10 07 February 2015

2. Artificial immune network model

2.1 *Natural immune system*

The natural immune system, which is made up of special cells, proteins and organs, protects organisms from infection with layered defenses of increasing specificity. Most simply, physical barriers prevent pathogens (called antigens, *g*) such as bacteria and viruses from entering the organism. One type of response is the secretion of antibody (*b*) molecules by B cells or B lymphocytes (Jerne 1973). When an antigen is detected, the B cells that recognize the antigen with best affinity will proliferate by cloning. Affinity represents the attraction between an antigen and an antibody. During reproduction, the B-cell clones undergo a hypermutation process where the antigen stimulates the B cell to proliferate and mature into terminal antibody-secreting cells that are named plasma cells. The activated B cells with high antigenic affinities are selected to become memory cells with long life spans (Zhong *et al.* 2006). These *memory cells* guarantee a faster response to similar antigens that may invade the organism in the future (Coelho and Von Zuben 2006).

To explain the memorial and learning capabilities exhibited by the immune system, immune network theory was proposed by Jerne (1974) and has been reviewed by Perelson (1989). It has been suggested that the immune system is composed of a regulated network of cells and molecules that recognize one another, even in the absence of antigens. In the artificial immune network, the immune cells can respond either positively or negatively to the recognition signal (antigen or other immune cell or molecule). A positive response results in cell proliferation, cell activation and antibody secretion, while a negative response leads to tolerance and suppression. The suppression mechanism guarantees the appropriate number of antibodies, from which one is removed if some suppression condition is satisfied, such as low affinity.

2.2 *Artificial immune network model*

As a novel artificial immune network model based on immune network theory, aiNet was proposed for performing data analysis and clustering tasks (De Castro and Von Zuben 2000, 2001). It generates a network of antibodies linked according to affinity (Euclidean distance in the feature space). A subset of the antibodies with the highest affinity with respect to a given antigen is selected and cloned proportionally to the affinity. All generated clones are mutated inversely to their affinity. A fixed percentage of clones is selected to be memory antibodies, by eliminating those whose affinity with the current antigen is less than a death threshold. If a pair of memory antibodies have an affinity greater than a suppression threshold, one of them is removed from the network (Galeano *et al.* 2005). The above process is illustrated in figure 1 by a simple clustering example (De Castro and Von Zuben 2001). As an illustration, suppose there is a dataset composed of three regions with a high density of data as shown in figure 1(*a*). A hypothetical network architecture generated by the learning algorithm to be presented is shown in figure 1(*b*). The numbers within the memory cells indicate their labels, the number next to the connections represents their strengths, and the dashed lines suggest connections to be pruned, in order to detect clusters and define the final network structure. It is worth noting that the total number of memory cells is generally higher than the number of clusters and much smaller than the number of samples.

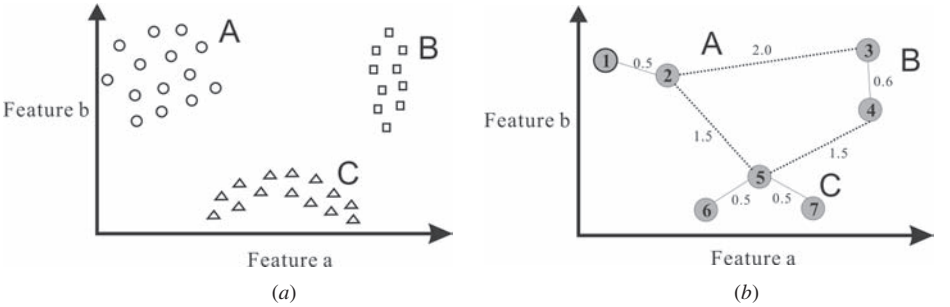

Figure 1. The principle of aiNet. (*a*) The dataset with three clusters (A, B, C) of high data density. (*b*) aiNetwork of labelled cells with their connection strengths assigned to the links. The dashed lines indicate connections to be pruned in order to generate disconnected sub-graphs, each characterizing a different cluster in the network (revised from De Castro and Von Zuben 2001).

Downloaded by [Wuhan University] at 19:10 07 February 2015

Many researchers have proposed different versions of immune network algorithms based on aiNet for different applications (Coelho and Von Zuben 2006) including opt-aiNet (Artificial Immune Network for Optimization; De Castro and Timmis 2002c, Timmis and Edmonds 2004), copt-aiNet as an extension of opt-aiNet for combinatorial optimization tasks (Gomes *et al.* 2003), dopt-aiNet (Artificial Immune Network for Dynamic Optimization; De Franca *et al.* 2005), Omni-aiNet (Artificial Immune Network for Omni-optimization; Coelho and Von Zuben 2006), and M-aiNet (modified aiNet; Campelo *et al.* 2006). In addition, aiNet has been applied to artificial neural network training (Pasti and De Castro 2006) and quantity and position determination of radial basis functions (RBFs) of the RBF neural network (De Castro and Von Zuben 2002).

These proposed aiNet or modified aiNet models have been applied successfully for data analysis, clustering and optimization; however, it is difficult to apply current aiNet series models to remote sensing image classification. The reasons are as follows: (*a*) current models require the storage and manipulation of a large network of B cells; (*b*) there are too many user-defined parameters in the current models – for example, clone rate and mutation rate usually need to be defined by the user; (*c*) the method of calculating the affinity in aiNet is not easily adapted to remote sensing image classification. The affinity is usually obtained by a reciprocal of the Euclidean distance in the feature space between the antigen and antibody to let the value lie within the range [0, 1] in these proposed network models; however, the value of affinity is very small because the Euclidean distance between two pixels in the feature space is often large in remote sensing image classification. That is, the affinity calculated by the Euclidean distance makes it difficult to make a distinction between good and bad antibodies or memory cells and (*d*) these current aiNet models do not have a parameter representing the number of classes. They often obtain the number of classes by analysing the clustering graph of all antibodies after the clustering process. The method is only effective when the feature-dimension is less than three because the visualization of higher dimensions is a difficult problem; however, the dimension of remote sensing images is often larger than three, for example seven bands in a Landsat TM image.

To overcome these obstacles and utilize the advantages of aiNet to improve the accuracy of image classification, this article proposes a novel unsupervised artificial immune network for remote sensing image classification (RSUAIN), based on aiNet.

Downloaded by [Wuhan University] at 19:10 07 February 2015

3. Unsupervised artificial immune network for remote sensing image classification

This section describes the proposed new classification method. At the end of the section, the new algorithm is compared to an earlier unsupervised artificial immune classifier (UAIC) (Zhong *et al.* 2006). RSUAIN addresses the above problems of aiNet as follows: (*a*) To decrease the number of B cells and memory cells, RSUAIN evolves the memory cell population after the evolution of each antigen, not after each iteration of aiNet. The proposed algorithm maintains the appropriate number of memory cells. (*b*) Some user-defined parameters, such as clone rate and mutation rate, are adaptively obtained in RSUAIN. (*c*) RSUAIN calculates the affinity based on the Spectral Angle Mapper (SAM) algorithm to adapt to the task of remote sensing image classification. (*d*) In RSUAIN, a parameter representing the number of classes is added.

The following notations are used to describe RSUAIN (Zhong *et al.* 2006):

- Let G and B denote the set of antigens and antibodies, with b and g representing a single antibody and a single antigen, respectively, where $b \in \mathrm{B}$ and $g \in \mathrm{G}$.
- Let M represent the set of memory cells or memory matrix and m represent an individual member of this set. M_c represents the memory cell's set of the cth class such that $\mathrm{M}_c \subseteq \mathrm{M} = \{\mathrm{M}_1 \cup \mathrm{M}_2 \cup \cdots \mathrm{M}_{nc}\}$ and $m \in \mathrm{M}_c = \{m \mid m.c \equiv c\}$.
- Let $g.c$ and $m.c$ represent the class of a given antigen and memory cell, g and m, respectively, where $m.c \in \mathrm{C}$ and $g.c \in \mathrm{C}$, $\mathrm{C} = \{1, 2, \ldots, n_\mathrm{c}\}$, n_c is the number of classes in the dataset.

The proposed algorithm is as follows.

3.1 *Initialization*

The initialization stage can be conceptualized as a data preprocessing stage combined with a parameter discovery stage (Zhong *et al.* 2006). RSUAIN selects randomly N_B antibodies from the G to constitute the B and applies the MaxMin algorithm (Katsavounidis 1994) to the initial memory cell population M from B. In this case, the initial memory cell population is obtained by the successive selection of representative instances until n_c memory cells have been found.

3.2 *Initial classification of* G *using RSUAIN*

The remote sensing image is classified according to the initial memory cell population. The attribute of the class of each antigen *ag* in the remote sensing image is assigned to the class of m, $g.c \equiv m.c \in$. $\mathrm{C} = \{1, 2, \ldots, n_\mathrm{c}\}$.

$$m = \arg\max_{m \in \mathrm{M}} \mathrm{affinity}(g, m) \tag{1}$$

A spectral angle mapper (SAM) (Kruse *et al.* 1993) is used to describe the feature space distance between two pixels, x and y, $\alpha(x, y)$. Let vector $x = (x^1, x^2, \ldots, x^{N_\mathrm{b}})$ and $y = (y^1, y^2, \ldots, y^{N_\mathrm{b}})$, where N_b is the band number of the remote sensing image. Then the distance between x and y is given by

$$\alpha(x, y) = \cos^{-1}\left\{ \frac{\sum_{i=1}^{N_\mathrm{b}} x^i y^i}{\left[\sum_{i=1}^{N_\mathrm{b}} (x^i)^2\right]^{1/2} \left[\sum_{i=1}^{N_\mathrm{b}} (y^i)^2\right]^{1/2}} \right\} \tag{2}$$

The smaller the spectral angle, $\alpha(x, y)$, the more similar the pixel and target spectrum.

Affinity is inversely proportional to distance in the feature space in artificial immune systems (De Castro and Timmis 2002a). RSUAIN uses a fuzzy affinity concept based on a fuzzy approach, $f(x, y)$, defined by equation (3) so that the affinity between antigens and antibodies or memory cells is in the range [0, 1]:

$$f(x, y) = \exp\left(-\frac{\alpha(x, y)}{2\sigma_i^2}\right) \tag{3}$$

Downloaded by [Wuhan University] at 19:10 07 February 2015

where σ_i is the scale or radius of influence in the feature space, which takes the experimental value of 1 in real applications.

According to equations (2) and (3), $\alpha(x, y) \in [0, \pi/2]$, and $f(x, y) \in [0.485, 1]$ with $\sigma = 1$.

3.3 *Iteration using RSUAIN*

Once initialization and initial classification are complete, the next step is the iteration of the algorithm. For each iteration, the algorithm performs the following steps to evolve each antigen g_j, $j = 1, \ldots, N_G$, ($g_j \in G$), in the remote sensing image, where N_G represents the number of image pixels.

The RSUAIN algorithm aims at building and evolving a memory matrix that recognizes and represents the remote sensing image. The evolution of memory matrix M_c ($g_j.c \equiv c$) is accomplished as follows.

3.3.1 Evolving the algorithm by recognizing the antigen g_j.

1. Calculate the affinity vector, f_j. Determine the vector f_j that contains the affinity of g_j to all the N_B antibodies, where N_B is the number of the antibody set B.
2. Select. Select the n highest affinity antibodies from B to compose a new antibody set of high affinity antibodies in relation to g_j, where n is the number of the cloned antibodies in B.
3. Clone. The n antibodies, selected independently and proportional to their antigenic affinities, generate a clone set C_E: unlike in UAIC, the number of clones for each antibody is no longer a free parameter, but instead is a fixed number $2n + 1$ to avoid the influence of variations in the number of clones (Campelo *et al*. 2006). The number of clones generated for all these n selected antibodies is given by

$$N_E = \sum_{i=1}^{n} (2n + 1) \tag{4}$$

   where N_E is the total number of clones generated for g.
4. Adaptive mutation. Submit the clones set C_E to an affinity maturation process inversely proportional to its antigenic affinity, generating a population C_E^* of matured clones: the higher the affinity, the smaller the mutation rate. The mutation rate is adaptively determined without user-definition as follows:

$$p_m = 1 - (f(g_j, b_i)/2) \tag{5}$$

   For each antibody b_i in the antibody population of the tth generation, create a mutated antibody b_i^* through non-uniform mutations as follows: if $b_i = \{v_1, \ldots, v_k, \ldots, v_{N_b}\}$ is a mutation and the element v_k is selected with the mutation rate p_m for this mutation, the result is a mutated antibody $b_i^* = \{v_1, \ldots, v_k', \ldots, v_{N_b}\}$ using the following equation (Zhao *et al.* 2007):

$$v_k' = \begin{cases} v_k + \Delta(t, U - v_k) & \text{if a random } \xi \text{ is 0,} \\ v_k - \Delta(t, v_k - L) & \text{if a random } \xi \text{ is 1} \end{cases} \tag{6}$$

Downloaded by [Wuhan University] at 19:10 07 February 2015

where ξ is a random number and L and U are the lower and upper bounds of the variable v_k, respectively. The function $\Delta(t,u)$ returns a value in the range [0, u] such that $\Delta(t,u)$ approaches to zero as m increases. This property allows this operator to search the space uniformly at early stages (when t is small), and very locally at later stages. The function $\Delta(t,u)$ is defined as

$$\Delta(t, u) = u\{1 - r^{[1-(t/\mathrm{T})]^{\lambda}}\} \tag{7}$$

where t is the iteration number, T is the maximal iteration number, r is a random value within the range [0,1], λ is a parameter to determine the nonconforming degree, for which the experiential value is in the range of [3, 5].

5. Recalculate. Re-determine the affinity f_j^* of the matured clones $\mathrm{C}_{\mathrm{E}}^*$ in relation to antigen g_j.
6. Reselect. From $\mathrm{C}_{\mathrm{E}}^*$, reselect $\zeta\%$ of the antibodies with higher affinity and put them into a candidate memory matrix M_m in the memory cell set M. This step is optional since the next step has the function of selection by the death of candidate memory cells.
7. Death. Remove the candidate memory cells in M_m whose affinities satisfy the inequality $f(b_k, g_j) < \sigma_{\mathrm{d}}$, where b_k represents the selected antibody and σ_{d} denotes the death rate which controls the affinity between the candidate memory cells and antigen. Only these candidate memory cells with the high affinity may go to the next evolving step.
8. Internal affinity calculation. Determine the affinity $f(b_i, b_l)$ between each two candidate memory cells, b_i and b_l in M_m using equation (3).
9. Suppression. Remove those candidate memory cells $f(b_i, b_l) > \sigma_{\mathrm{s}}$ to reduce the size of the M_m matrix and maintain the diversity of the memory cell pool. σ_{s} represents the suppression rate. Then, output the resultant clonal memory matrix M_m^*. The class attribute of all the memory cells in M_m^* is equal to the class attribute of g_j, $\mathrm{M}_m^*.c = g_j.c \equiv c$.
10. Concatenate the total memory cell matrix with the resultant clonal memory M_m^* for g_j: $\mathrm{M} \leftarrow [\mathrm{M}; \mathrm{M}_m^*]$. These candidate memory cells become the memory cells in the next step.
11. Internal re-calculation and re-suppression. Repeat step (8) and step (9) to M to reduce the size of M_c, which has the same class attribute as g_j.

Once step (11) has been accomplished, the recognition of this antigen has been completed. The next antigen in the remote sensing image is selected and the process proceeds from step (1) to (11) until the system has been presented with all antigens in the image, that is, all pixels in the image have been evolved.

3.3.2 Updating the memory matrix M. After step 3.3.1, the algorithm may obtain the memory matrix M of all classes. To maintain the size of the memory cell pool, the M is suppressed by the following steps:

1. Internal calculation in M. Determine the affinity $f(m_i, m_l)$ between two memory cells in M using equation (3).
2. Network suppression. Remove those memory cells $f(m_i, m_l) > \sigma_{\mathrm{s}}$ to reduce the size of M by considering the influence of the classes because the memory cell M has the class attribute, $\mathrm{M} = \{\mathrm{M}_1 \cup \mathrm{M}_2 \cup \cdots \cup \mathrm{M}_{n_c}\}$.

Downloaded by [Wuhan University] at 19:10 07 February 2015

3.3.3 Classification of G using the new memory cell matrix M. By step 3.3.2, a new memory cell matrix M has been obtained. The classification of G is performed according to step 3.2, in which each antigen is determined to the same class of the memory cell with the maximal affinity to g.

3.3.4 Update the antibody population. The d new antibodies are produced by a random process from the G to replace the old antibodies. These old antibodies are selected according to their affinities, and RSUAIN often selects the d old antibodies with lower affinity. This step may increase the diversity of the antibody population, B. To reduce the parameters, d can be obtained by the following equation:

$$d = N_{\mathrm{B}} \times \zeta\% \tag{8}$$

Once the memory matrix and the memory cell sets M have been suppressed, this iteration is complete.

3.4 *Stopping condition*

When the number of iterations reaches the user-defined number or the change of memory cells between two consecutive iterations is less than a change threshold, the execution of the algorithm is terminated. Otherwise, return to step 3.3 until the stop criteria are satisfied.

Finally, RSUAIN outputs the result of the classification of the remote sensing image.

3.5 *Comparision with earlier unsupervised artificial immune classifier*

In previous work, an unsupervised artificial immune classifier (UAIC) has been proposed and been applied for the classification of remote sensing imagery (Zhong *et al*. 2006). Unlike RSUAIN, UAIC is characterized mainly by immunological properties, such as clonal selection theory and immune memory, and does not utilize immune network theory (table 1). Compared with the concept of antibodies in aiNet, UAIC proposes the AB (antibody) model to describe the antibody population in immune systems that contain many antibodies of the class and memory cells, with every AB model being able to recognize all antigens in its scale/radius of influence. In addition to the updating of the memory cell population, UAIC uses the distance threshold scalar (DTS) to update the memory cells and control the number of memory cells in the population, but RSUAIN defines two parameters, death rate σ_{d} and suppression rate σ_{s}, to update the memory cell matrix, and to specify which network cells are connected to each other describing the general network structure (see also section 3). In RSUAIN, each class has an inner network connection, and the affinity of these memory cells is less than the suppression rate σ_{s} to maintain the diversity of the memory cell population. The diversity can let RSUAIN approximate any function with arbitrary accuracy by a universal functional approximator to improve the classification accuracy.

Downloaded by [Wuhan University] at 19:10 07 February 2015

Table 1. Comparison between an unsupervised artificial immune classifier (UAIC) and a remote sensing unsupervised artificial immune network (RSUAIN).

Aspects	UAIC (Zhong *et al*. 2006)	RSUAIN
Principle	Clonal selection algorithm, immune memory, etc.	Immune networks
Model	Antibody (AB) model	aiNet and memory matrix
Affinity	Spectral angle mapping algorithm	Spectral angle mapping algorithm
Network	None	Memory cell matrix
Candidate memory cell	Antibody with the highest affintiy	Antibodies with affinities larger than death rate σ_d
Controlling parameters	Distance threshold (DT) and distance threshold scalar (DTS)	Death rate σ_d and suppression rate σ_s
Mutation operator	Gaussian mutation	Non-uniform mutation

Downloaded by [Wuhan University] at 19:10 07 February 2015

4. Experiments and analysis

The proposed RSUAIN and traditional unsupervised algorithms were implemented and tested on different types of remote sensing images. Three experiments were conducted to test the performance of classification. Comparisons were also carried out between RSUAIN and *k*-means, ISODATA, fuzzy *k*-means, and UAIC in all experiments.

4.1 *Experiment 1: Flightline C1*

This experiment was conducted using a dataset designated Flightline C1 (FLC1), which consists of 12-band multispectral data taken over Tippecanoe County, IN, by the Multispectral Airborne Scanner M7 in June 1966 (Tadjudin and Landgrebe 2000). For convenient comparison with the unsupervised algorithms, we used part of the dataset (190 × 110 pixels) with a spectral range from 0.40 to 1.00 μm (bands 1–12). Figure 2(*a*) shows the FCL1 image. The survey area is an agricultural district, and the primary objective of the survey was to achieve land cover classification. The observed image was expected to fall into four classes: soy, wheat, red clover and oats. The list of classes and the number of labelled samples for each class are given in table 2. The field map, based on ground reference data, is shown in figure 2 (*b*).

The primary parameters specified by the user for the classification are the number of classes n_c, the maximum iterations T, antibody population size N_B, death rate σ_d, suppression rate σ_s, the number of selected antibodies n, and the reselect rate $\zeta\%$. Here, n_c is equal to four because the image was expected to fall into four classes. The values of parameters were set by experience as: $T = 10$, $N_B = 100$, $n = 10$, $\zeta\% = 10\%$. These values of σ_d and σ_s were selected from a sensitivity analysis (see section 5), $\sigma_d = 0.96$, $\sigma_s = 0.92$. According to equation (8), $d = N_B \times \zeta\% = 100 \times 10\% = 10$. For convenient comparison between RSUAIN and the traditional unsupervised algorithms, the change threshold and the maximum iteration as stop conditions were kept at the same values, namely 3% and 10. The parameters of ISODATA were set as follows: number of initial classes = 4, minimum number of pixels in class = 1,

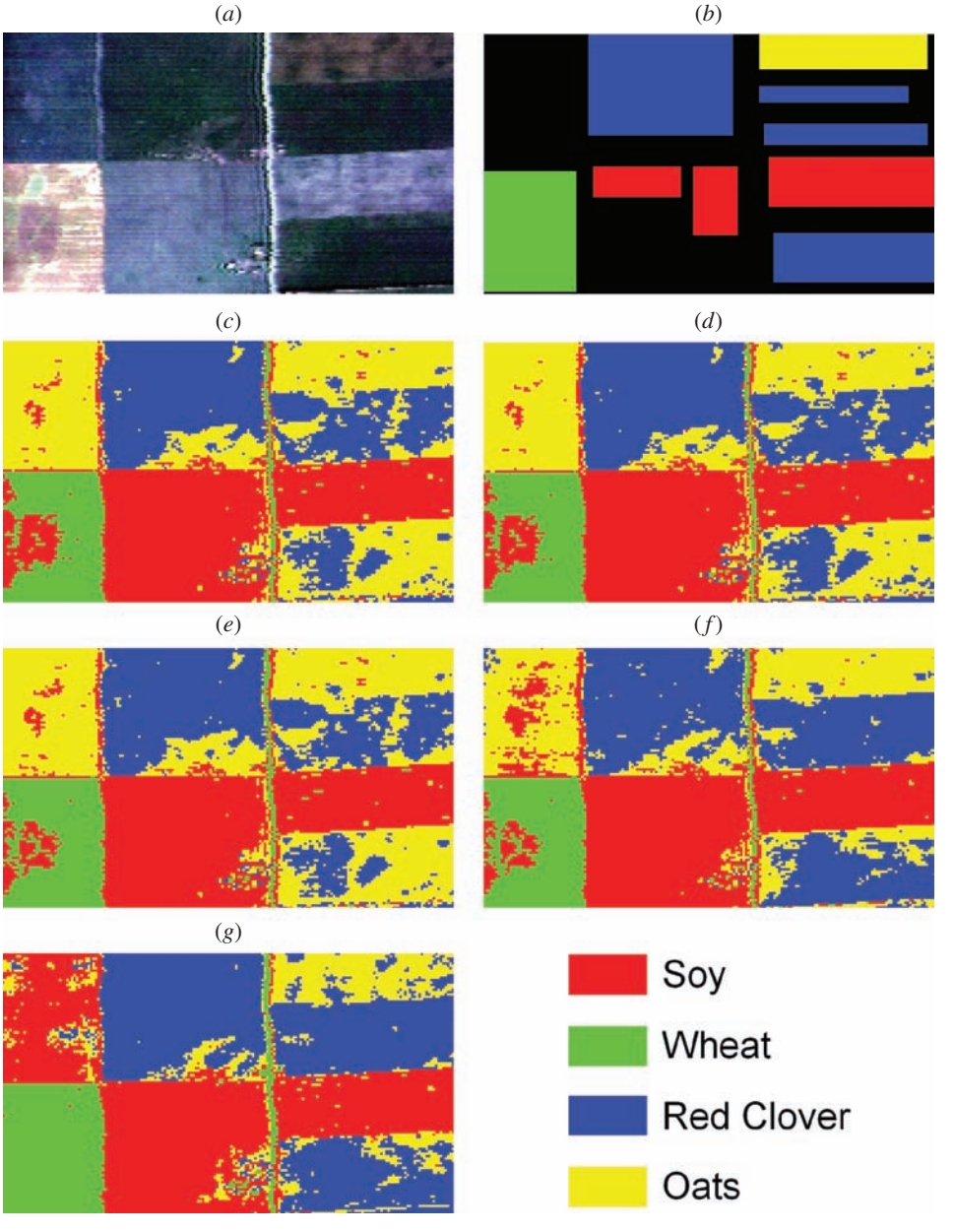

Figure 2. Unsupervised classification images for Flight C1 image. (*a*) Flightline C1 Image as RGB (bands 9, 7, 4), (*b*) ground reference data of FLC1, (*c*) *k*-means, (*d*) Iterative Self-organizing Data Anaysis Techniques Algorithm (ISODATA), (*e*) fuzzy *k*-means, (*f*) unsupervised artificial immune classifier (UAIC), (*g*) remote sensing unsupervised artificial immune network (RSUAIN).

maximum class standard deviation = 1.00, minimum class distance = 5.00, maximum merge pairs = 2. In addition, the parameters of fuzzy *k*-means were set as follows: weighting exponent $m = 2$, which is the optimal range of m within [1.5, 2.5] in the practical applications (Pal and Bezdek 1995). All the available samples were used as the evaluating dataset.

Downloaded by [Wuhan University] at 19:10 07 February 2015

Table 2. Classes and number of labelled samples for Experiment 1.

Class name	Number of labelled samples
Soy	2502
Wheat	1989
Red clover	5113
Oats	1065
Total number of samples	10 669

Figures 2(*c*)–(*g*) illustrate the classification results using *k*-means, ISODATA, fuzzy *k*-means, UAIC and RSUAIN. The visual comparison of the five unsupervised classifications in figure 2 shows varying degrees of accuracy in pixel assignment. The five classifiers have similar classification results for the soy class. For the wheat and oats classes, *k*-means, ISODATA, fuzzy *k*-means, and UAIC have similar results. RSUAIN and UAIC appear to have the better results for the red clover than other classifiers. Compared with UAIC, RSUAIN is more accurate for the wheat class than UAIC and other traditional classifiers since some wheat pixels are misclassified as the soy class at the bottom left of the classification image obtained by the other four algorithms. In summary, RSUAIN gives higher accuracy for all four classes.

After executing RSUAIN, the number of memory cells and the internal affinity matrix of memory cells in the output constructed network can be obtained, as shown in tables 3 and 4, respectively. Figure 3 shows the spectral curves of seven memory cells. It should be noted that the number of memory cells in each class is highly correlated to the parameters of death rate σ_d and suppression rate σ_s, where σ_d controls the number of candidate memory cells and indirectly the number of final memory cells (see also step 7 in section 3.3.1), while σ_s controls directly the number of memory cells

Table 3. The number of memory cells in each class for Experiment 1.

Class name	Number of memory cells
Soy	1
Wheat	2
Red clover	2
Oats	2
Total	7

Table 4. The internal affinity matrix of memory cells in the output constructed network.

Matrix	Soy	Wheat1	Wheat2	Red clover1	Red clover2	Oats1	Oats2
Soy	–	0.918	0.936	0.849	0.915	0.919	0.961
Wheat1	–	–	0.920	0.789	0.851	0.870	0.887
Wheat2	–	–	–	0.807	0.863	0.874	0.915
Red clover1	–	–	–	–	0.920	0.889	0.872
Red clover2	–	–	–	–	–	0.933	0.936
Oats1	–	–	–	–	–	–	0.920
Oats2	–	–	–	–	–	–	–

Downloaded by [Wuhan University] at 19:10 07 February 2015

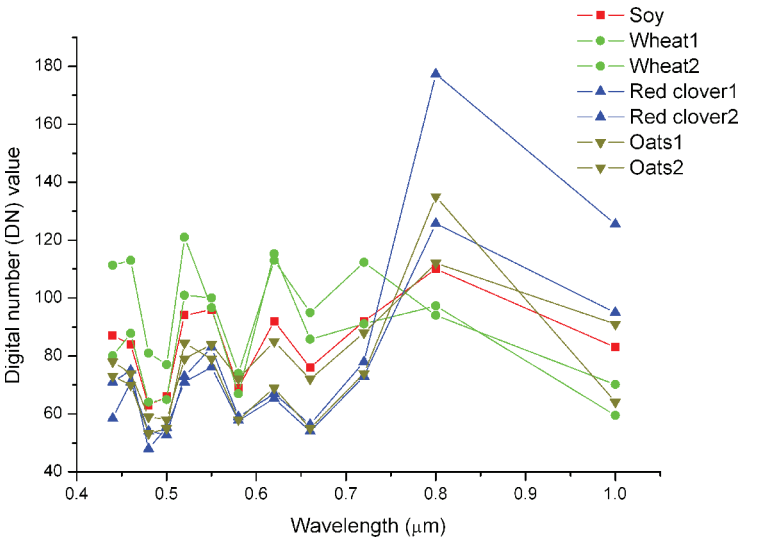

Figure 3. The spectral curves of all memory cells in Experiment 1.

(see also step 9 in section 3.3.1 and step 2 in section 3.3.2). The sensitivity analysis of σ_d and σ_s will be described in detail in section 5.

For a more detailed verification of the results, the ground reference data (table 2) were compared with the classified images and the accuracy of each classifier was quantitatively assessed using four statistics: producer's accuracy, user's accuracy, overall accuracy (OA), and Kappa coefficient based on the confusion matrix (Campbell 2000). To evaluate the statistical reliability of the classification results, statistical tests of significance need to be performed. The classifier was run on the 10 testing sets of each dataset to produce the corresponding classification accuracy. The 10 classification accuracies were averaged to yield an overall classification performance of the proposed algorithm. Due to the fact that RSUAIN is evolutionary and the results obtained are unlikely to be similar twice, i.e. RSUAIN is non-deterministic, the experiment described above was performed 10 times by the 10×10-fold cross validation technique. The results obtained were again averaged.

Table 5 lists the results of the comparisons between the ground reference data and the classified images obtained by five unsupervised classifiers: *k*-means, ISODATA, fuzzy *k*-means, UAIC and RSUAIN. From table 5, it is apparent that the RSUAIN classifier produces better classification results than the other classifiers. The details are as follows: the five classifiers have similar results for the soy class. RSUAIN achieves better classification results for the wheat and red clover classes than the three traditional classifiers and UAIC, while these classifiers may slightly exceed RSUAIN in the oats class. As a whole, RSUAIN exhibits the best overall classification accuracy of 95.3% with a gain of 13.7%, 12.1%, 13.0% and 3.6% over the *k*-means, ISODATA, fuzzy *k*-means, and UAIC algorithms, respectively. RSUAIN improves the Kappa coefficient from 0.74 to 0.93, an improvement of 0.19. This is due to the conventional unsupervised classifiers often becoming stuck at suboptimal solutions based on the initial configuration of their systems, and they have low precision. RSUAIN and UAIC are inspired by immune systems, and are also data-driven, self-adaptive methods that can adjust themselves to the data without any explicit specification of functional or

Downloaded by [Wuhan University] at 19:10 07 February 2015

Table 5. Comparison of classifier performance in Experiment 1.

Methods	Classes	*k*-means	ISODATA	Fuzzy *k*-means	UAIC	RSUAIN
Producer's accuracy (%)	Soy	98.7	98.5	98.8	99.4	98.6
	Wheat	74.0	75.6	82.8	84.2	99.9
	Red clover	73.1	76.2	70.9	89.7	94.4
	Oats	96.5	95.1	97.3	97.1	83.9
User's accuracy (%)	Soy	82.3	83.2	87.3	88.7	99.7
	Wheat	99.7	99.5	99.5	99.8	99.9
	Red clover	99.4	99.0	99.6	99.4	96.5
	Oats	42.3	44.90	40.7	65.7	74.0
Overall accuracy (%)		81.6	83.2	82.3	91.7	95.3
Kappa		0.74	0.76	0.75	0.88	0.93

ISODATA, Iterative Self-organizing Data Anaysis Techniques Algorithm; UAIC, unsupervised artificial immune classifier; RSUAIN, remote sensing unsupervised artificial immune network.

Downloaded by [Wuhan University] at 19:10 07 February 2015

distributional form for the underlying model. Compared with UAIC, RSUAIN controls the number of memory cells in each of the classes by the parameters of death rate and suppression rate, where death rate controls the number of candidate memory cells to improve the affinity of memory cells, while suppression rate controls directly the number of memory cells. RSUAIN can generate optimal centroids of clusters by the constructed network using the above controlled parameters. Based on the above, we can conclude that RSUAIN has a better performance than other classification methods in this study.

4.2 *Experiment 2: Wuhan TM*

This experiment was conducted using a Landsat Thematic Mapper (TM) image dataset with 30 m pixels. The image (400 × 400 pixels) shown in figure 4(*a*) was acquired of Wuhan city, Hubei, China, on 26 October 1998 with bands 1 (0.45–0.52 μm), 2 (0.52–0.60 μm), 3 (0.62–0.69 μm), 4 (0.76–0.96 μm), 5 (1.55–1.75 μm) and 7 (2.08–3.35 μm) being employed (Zhong *et al.* 2006). The survey area is part of the city, and the primary objective of the survey was to discriminate four classes: water (including the famous Yangtse River), vegetation, bare land/road (including paved and unpaved roads) and urban areas. The list of classes and the number of labelled samples for each class are given in table 6. The ground reference data used to evaluate the classification accuracy are shown in figure 4(*b*). The ground reference data include that of Zhong *et al.* (2006) supplemented by additional field mapping to increase the statistical reliability of the classification results.

Table 6. List of classes and number of labelled samples in each class for Experiment 2.

Class name	Number of labelled samples
Water	4025
Vegetation	5830
Bare land/Road	2763
Urban area	2512
Total number of samples	15 130

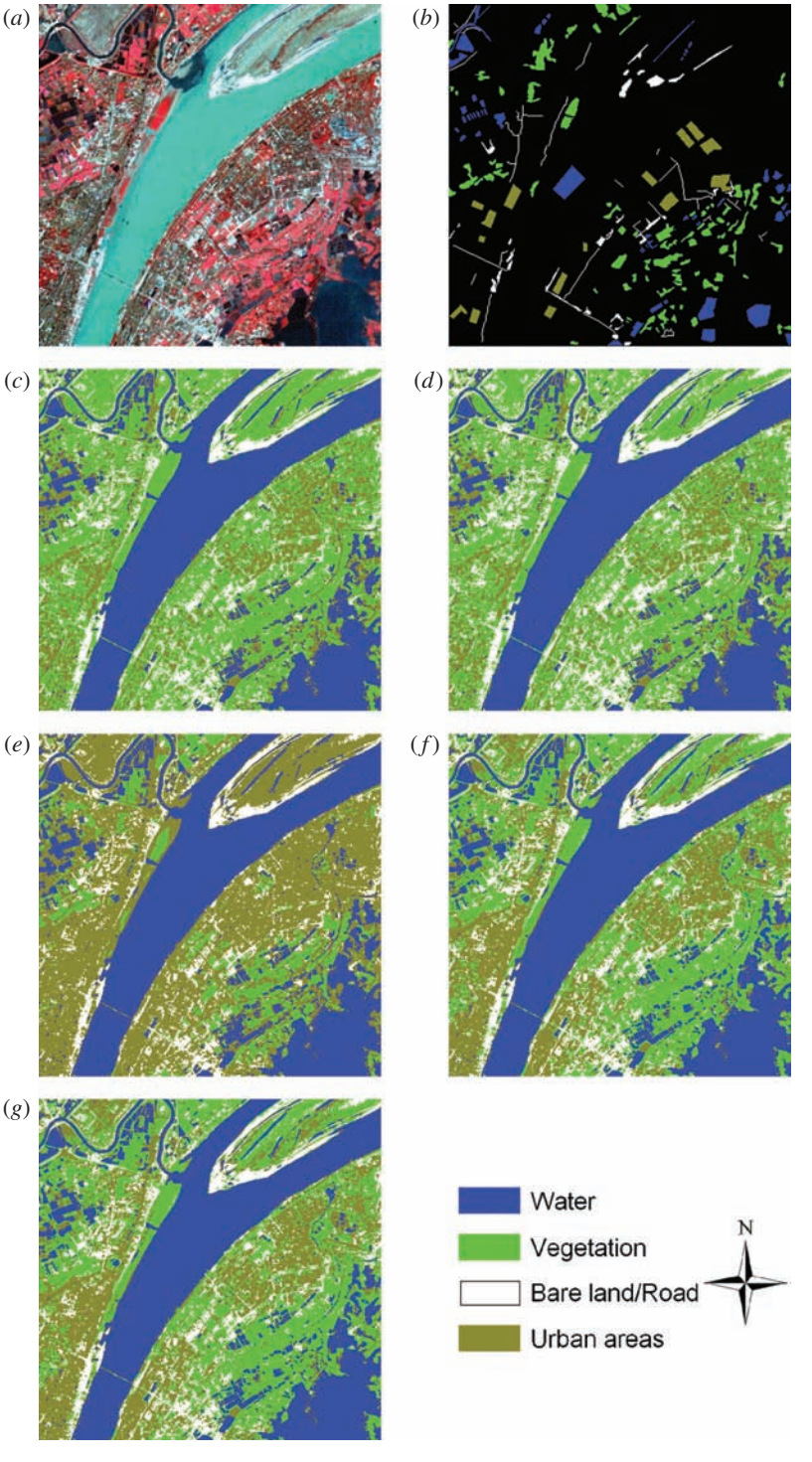

Figure 4. The classification images for Wuhan Thematic Mapper (TM) image in Experiment 2. (*a*) Wuhan TM Image as RGB (bands 4, 3, 2), (*b*) ground reference data, (*c*) *k*-means, (*d*) Iterative Self-organizing Data Anaysis Techniques Algorithm (ISODATA), (*e*) fuzzy *k*-means, (*f*) unsupervised artificial immune classifier (UAIC), (*g*) remote sensing unsupervised artificial immune network (RSUAIN).

Downloaded by [Wuhan University] at 19:10 07 February 2015

Table 7. Comparison of classifier performance in Experiment 2.

Methods	Classes	*k*-means	ISODATA	Fuzzy *k*-means	UAIC	RSUAIN
Producer's accuracy (%)	Water	89.4	92.2	95.5	96.9	97.6
	Vegetation	67.0	67.2	67.5	71.7	76.4
	Bare land/Road	65.4	61.4	64.2	75.4	78.9
	Urban area	71.7	83.5	85.0	94.4	91.5
User's accuracy (%)	Water	97.0	97.0	97.1	98.1	99.5
	Vegetation	83.3	96.3	96.0	97.3	99.1
	Bare land/Road	57.7	56.4	58.7	69.5	71.7
	Urban area	51.1	51.3	54.2	63.5	64.5
Overall accuracy (%)		73.6	75.9	77.6	83.2	85.2
Kappa		0.64	0.68	0.70	0.77	0.80

Note: ISODATA, Iterative Self-organizing Data Anaysis Techniques Algorithm; UAIC, unsupervised artificial immune classifier; RSUAIN, remote sensing unsupervised artificial immune network.

Downloaded by [Wuhan University] at 19:10 07 February 2015

The values of the classification parameters were set as: $n_c = 4$, $T = 10$, $N_B = 100$, $n = 10$, $\zeta\% = 10\%$, $\sigma_d = 0.98$, $\sigma_s = 0.92$. According to equation (8), $d = N_B \times \zeta\% = 100 \times 10\% = 10$. The parameters of the other traditional algorithms are the same as in Experiment 1.

Figures 4(*c*)–(*g*) illustrate the classification results using *k*-means, ISODATA, fuzzy *k*-means, UAIC and RSUAIN algorithms, respectively. The classification accuracies for the classifiers, calculated overall accuracy and Kappa coefficient, are given in table 7.

The visual comparisons of the five cluster classifications in figure 4 suggest varying degrees of accuracy of classification, similar to those in Zhong *et al.* (2006). The five classifiers have similar classification results for the water class. *k*-means and ISODATA create similar classification maps, with poor differentiation between urban areas and bare land/roads. In contrast, fuzzy *k*-means distinguishes well between urban areas and bare land/roads, but has the lowest vegetation classification accuracy with many vegetation pixels misclassified as the urban area class. By contrast, RSUAIN and UAIC appear to achieve better accuracy in the vegetation class than the other classifiers, and also perform satisfactorily in the urban area and bare land/road classes based on a visual comparison. As a result, RSUAIN and UAIC appear to obtain better results than other traditional classifiers. This qualitative finding is supported by the quantitative analysis (table 7). The details are as follows: RSUAIN has the highest overall classification accuracy of 85.2% compared to 73.6% for *k*-means, and 83.2% for UAIC, an improvement of 11.6% and 2%, respectively. The Kappa coefficient increases from 0.64 for *k*-means to 0.80 for RSUAIN, an improvement of 0.16. The slight difference in classification results compared to those of Zhong *et al.* (2006) is due to the greater number of test samples added by field collection in the method described in this article. Based on the above, RSUAIN outperformed the other four techniques in this study.

4.3 *Experiment 3: Indian Pine AVIRIS*

Experiment 3 was performed using a portion of an Airborne Visible/Infrared Imaging Spectrometer (AVIRIS) dataset taken over Northwest India's Indian Pine test in June

Table 8. List of classes and number of labelled samples in each class for Experiment 3.

Class name	Number of labelled samples
Corn-no-till	1008
Grass	747
Soybeans-no-till	737
Soybeans-minimum-till	1947
Total number of samples	4439

1992 (Tadjudin and Landgrebe 2000). The scene contains four known information classes: Corn-no-till, Grass, Soybeans-no-till, Soybeans-minimum-till (table 8). By visual inspection of the image, the list of these ground cover types is assumed to be exhaustive. A total of 20 channels from the water absorption and noisy bands (104–108, 150–163, 220) were removed from the original 220 spectral channels, leaving 200 spectral features for the experiments. The original image data and the ground reference map are shown in figures 5(*a*) and (*b*).

Downloaded by [Wuhan University] at 19:10 07 February 2015

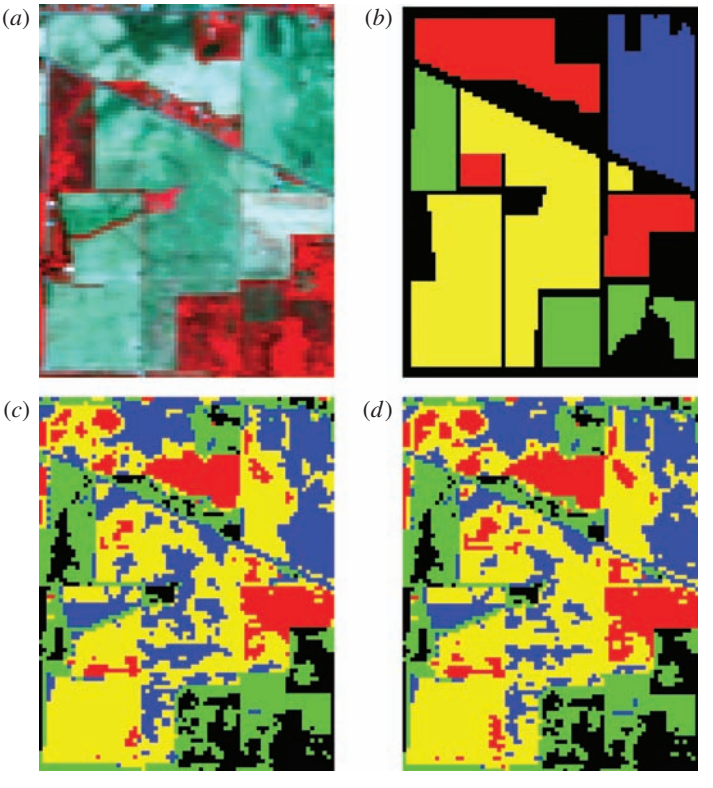

Figure 5. The classification images for Airborne Visible/Infrared Imaging Spectrometer (AVIRIS) image in Experiment 3. (*a*) AVIRIS image, (*b*) ground reference data, (*c*) *k*-means, (*d*) Iterative Self-organizing Data Anaysis Techniques Algorithm (ISODATA), (*e*) fuzzy *k*-means, (*f*) unsupervised artificial immune classifier (UAIC), (*g*) remote sensing unsupervised artificial immune network (RSUAIN).

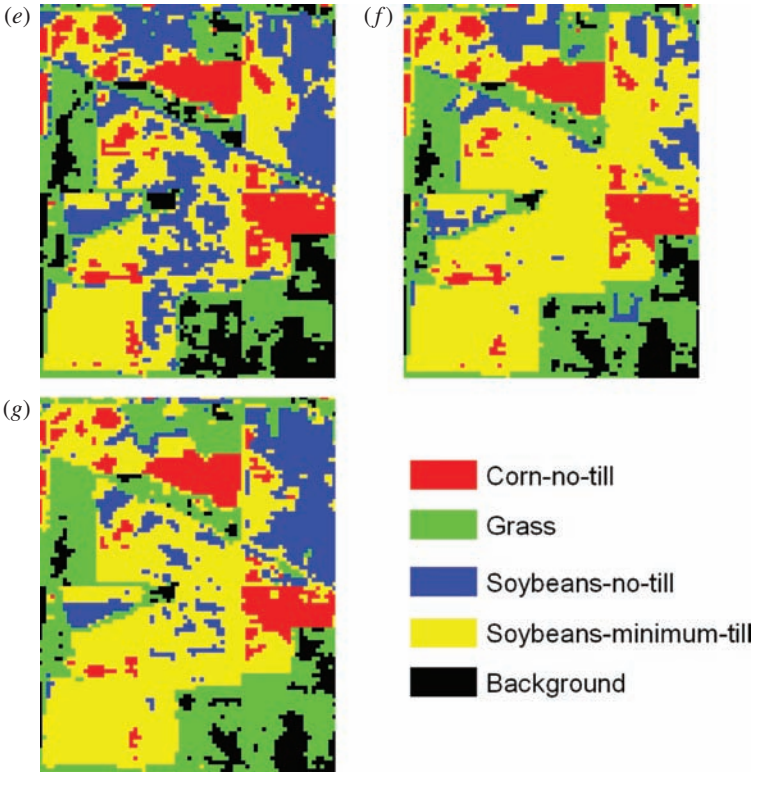

Figure 5. (*Continued*).

To test the classifier performance, the optimal number of clusters was assumed as the number of clusters using the Xie–Beni index, cluster validation method (Xie and Beni 1991). The number of clusters was set to five. The values of parameters were set as: $n_c = 5$, $T = 20$, $N_B = 100$, $n = 10$, $\zeta\% = 10\%$, $\sigma_d = 0.98$, $\sigma_s = 0.92$. According to equation (8), $d = N_B$.

Figures 5(*c*)–(*g*) illustrate the classification results using *k*-means, ISODATA, fuzzy *k*-means, UAIC and RSUAIN algorithms, respectively. The classification accuracies for the classifiers, calculated using overall accuracy and Kappa coefficient, are given in table 9. As shown in figure 5 and table 9, *k*-means and fuzzy *k*-means have similar classification results, and there is obvious misclassification between the Soybeans-no-till class and Soybeans-minimum-till class becasuse of their similar spectral responses. The ISODATA has a lower number of misclassified pixels, with some Soybeans-minimum-till pixels being classified correctly in the centre of the classification image. The UAIC has the best classification results for the Soybeans-minimum-till class (88.2%), while the Soybeans-no-till class is not classified correctly. Compared with other classifiers, RSUAIN does not have the best classification accuracy for each class, but it has the best visual and overall accuracy (73.8%), and also performs satisfactorily for the Soybeans-no-till and Soybeans-minimum-till classes. It is worth noting that RSUAIN and UAIC have better classification results than traditional classifiers, but UAIC has the worst result for the Soybeans-no-till class with some Soybeans-no-till pixels misclassified to the Soybeans-minimum-till class. These results may be a consequence of the fact that UAIC has many memory cells of Soybeans-minimum-till

Downloaded by [Wuhan University] at 19:10 07 February 2015

Table 9. Comparison of classifier performance in Experiment 3.

Methods	Classes	*k*-means	ISODATA	Fuzzy *k*-means	UAIC	RSUAIN
Producer's accuracy (%)	Corn-no-till	46.7	51.7	51.2	47.4	43.6
	Grass	98.9	98.1	99.2	95.0	99.9
	Soybeans-no-till	53.9	50.3	55.2	23.4	72.1
	Soybeans-minimum-till	66.0	70.1	60.8	88.2	81.2
User's accuracy (%)	Corn-no-till	80.9	75.2	75.8	80.1	83.1
	Grass	93.0	92.3	92.0	94.0	82.4
	Soybeans-no-till	34.4	34.0	33.4	39.0	63.3
	Soybeans-minimum-till	66.9	68.5	67.5	65.2	72.4
Overall accuracy (%)		63.4	65.7	62.1	68.6	73.8
Kappa		0.47	0.50	0.46	0.52	0.62

ISODATA, Iterative Self-organizing Data Anaysis Techniques Algorithm; UAIC, unsupervised artificial immune classifier; RSUAIN, remote sensing unsupervised artificial immune network.

Downloaded by [Wuhan University] at 19:10 07 February 2015

classes, and many Soybeans-no-till pixels are misclassified because of the similarity of the Soybeans-no-till and Soybeans-minimum-till classes. RSUAIN uses the death date and suppression rate to update the memory cell population, while keeping the good recognition rate for the antigen (unclassified pixel). As a result, RSUAIN has better results than other classifiers in this experiment.

5. Sensitivity analysis of RSUAIN

RSUAIN has two important user-defined parameters that significantly influence the classification: (1) the number of final memory cells; and (2) the computational complexity. These parameters are as follows.

1. Death rate σ_d: controls the affinity levels and the number of candidate memory cells, with their affinity being greater than σ_d, and indirectly the number of final memory cells (see also step 7 in section 3.3.1).
2. Suppression rate σ_s: controls directly the number of memory cells and maintains the diversity of the memory cell pool (see also step 9 in section 3.3.1 and step 2 in section 3.3.2).

In order to analyse the effects of setting these parameters when running RSUAIN, the Landsat TM image, shown in figure 4(*a*), was classified using different values for the parameters. Each experiment was performed 10 times and the results obtained were averaged.

5.1 *Sensitivity in relation to parameter* σ_d

Death rate σ_d controls the affinity between candidate memory cells and the antigen to determine the quality of memory cells and indirectly the number of candidate memory cells. Only if the affinity between one antibody and antigen is larger than σ_d can the antibody have a chance of becoming a candidate memory cell or a final memory cell. In order to study the RSUAIN sensitivity in relation to death rate σ_d, other parameters were kept the same as in Experiment 1 with $\sigma_s = 0.92$ but σ_d assuming the following values: $\sigma_d = \{0.95, 0.96, 0.97, 0.98\}$. Figure 6 illustrates the sensitivity of RSUAIN accuracy and number of memory cells on the parameter σ_d.

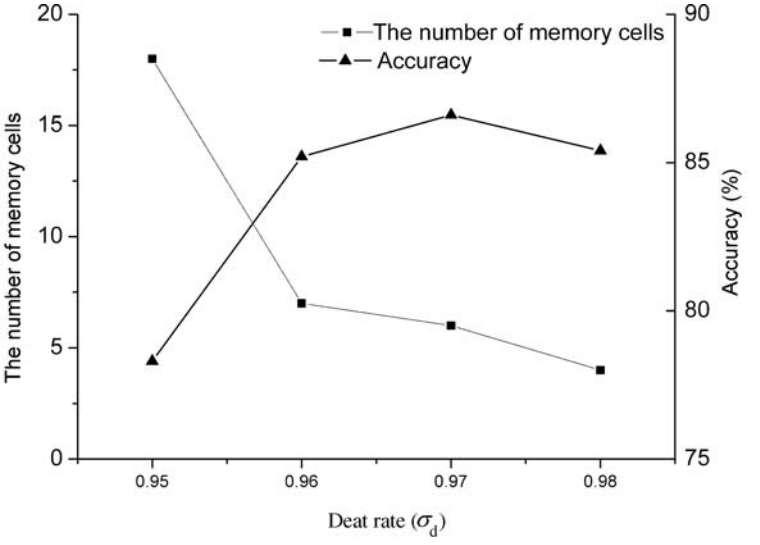

Figure 6. Sensitivity of remote sensing unsupervised artificial immune network (RSUAIN) in relation to σ_d.

As shown in figure 6, when the other parameters are fixed, the smaller the value of σ_d, the greater the number of memory cells. The overall accuracy increases when the value of σ_d is changed from 0.95 to 0.97 and it reaches a maximum, 86.6%, with the overall accuracy decreasing as the value of σ_d increases. The reason is as follows: when σ_d is small, more antibodies may become candidate memory cells because their affinities satisfy the inequality $f > \sigma_d$ (see also step 7 in section 3.3.1). The increase in the number of candidate memory cells improves the probability, so that the candidate memory cells become the final memory cells. That is, the value of σ_d indirectly influences the number of final memory cells. However, too many memory cells does not improve the classification accuracy by decreasing the value of σ_d; it may even decrease the accuracy because the final memory cells do not correctly represent the whole antigen population, as the error between these memory cells and the antigen may be too large. In addition, too large a σ_d may lead to too few candidate memory cells, while those candidate memory cells obtained also cannot represent the original antigen set. In real applications, the value of σ_d is defined by the user according to different requirements.

5.2 *Sensitivity in relation to parameter* σ_s

σ_s controls the number of memory cells and the diversity of the memory cell pool. In order to study the RSUAIN sensitivity in relation to the death rate σ_s, other parameters were kept the same as in Experiment 2, except for the death rate $\sigma_d = 0.96$ and σ_s assumed the following values: $\sigma_s = \{0.90, 0.91, 0.92, 0.93, 0.94, 0.95, 0.96\}$ as seen in figure 7.

As shown in figure 7, the number of memory cells increases from 4 to 48 when σ_s increases from 0.90 to 0.96. For the value $\sigma_s = 0.90$, the number of memory cells is equal to the number of classes, four. It is also interesting to observe that the number of memory cells increases quickly from 22 to 48, an increase of nearly 100%. Too

Downloaded by [Wuhan University] at 19:10 07 February 2015

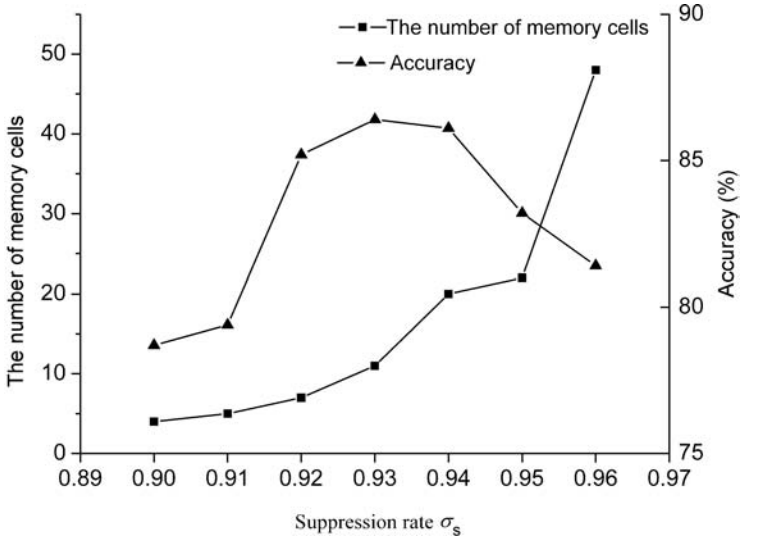

Figure 7. Sensitivity of remote sensing unsupervised artificial immune network (RSUAIN) in relation to σ_s.

large a σ_s leads to the reduction of the memory cell population's diversity since the population will become a mass with many memory cells, which can reduce the classification accuracy. For instance, when σ_s is equal to 0.96, the accuracy is only 81.4%. In contrast, a small value of σ_s (i.e. 0.90) also has negative effects, in that each class may only obtain one memory cell resulting in low classification accuracy (78.7% with $\sigma_s = 0.90$). Based on our experience and experiments, optimum values for σ_s typically range between 0.91 and 0.95.

6. Conclusions

This article describes an artificial immune approach for unsupervised classification of remote sensing image data. The unsupervised classification approach, RSUAIN, is developed for remote sensing image classification based on the paradigm of artificial immune network models, i.e. artificial immune network (aiNet). RSUAIN overcomes the disadvantages of aiNet, for example the need for many user-defined parameters, and was successfully applied to the classification of remote sensing images. RSUAIN is capable of performing data clustering by utilizing the advantages of aiNet, for instance the nonlinear model and immune memory, to generate an immune memorial network for classification. Two key user-defined parameters, death rate σ_d and suppression rate σ_s, determine the above process. The article provides a sensitivity analysis of RSUAIN in relation to the two parameters to allow users to improve the effectiveness of the algorithm according to different real applications.

Three experiments were carried out to test the performance of RSUAIN using aerial and satellite multispectral remote sensing images. Compared with three traditional unsupervised classifiers, *k*-means, ISODATA and fuzzy *k*-means, RSUAIN showed greater accuracy in the two case studies, for the experimental conditions chosen. In the experiments, the average RSUAIN classification overall accuracy improved to 84.8% compared to 72.9% using *k*-means, 74.9% using ISODATA, and 74.0% using fuzzy

Downloaded by [Wuhan University] at 19:10 07 February 2015

k-means; and the average Kappa coefficient improved to 0.78 with RSUAIN compared to 0.62 using *k*-means, 0.65 using ISODATA, and 0.64 using fuzzy *k*-means. The improvement of overall accuracy and Kappa coefficient is 11.9% and 0.16, respectively. RSUAIN also has better classification results than UAIC, which obtained higher classification accuracy than three traditional classifiers. It is worth noting that the difference in accuracy between UAIC and RSUAIN is largest in Experiment 3 when the spectral dimension of the remote sensing image is very high (i.e. 200). This evidences that RSUAIN is capable of performing the task of remote sensing image classification and has high classification precision. In future work we will integrate fuzzy theory for improving the classification performance.

Acknowledgements

The authors thank the editor and the two anonymous reviewers. Their insightful suggestions have significantly improved this article. This work is supported by the Major State Basic Research Development Programme (973 Programme) of China under Grant No. 2009CB723905, the 863 High Technology Programme of the People's Republic of China under Grant No. 2009AA12Z114, the National Natural Science Foundation of China under Grant Nos 40901213 and 40930532, the Foundation for Authors of National Excellent Doctoral Dissertations (FANEDD) of the People's Republic of China under Grant No. 201052, the Research Fund for the Doctoral Programme of Higher Education of China under Grant No. 200804861058, the Programme for New Century Excellent Talents in University under Grant No. NECT-10-0624, the Natural Science Foundation of Hubei Province under Grant No. 2009CDB173, the Fundamental Research Funds for the Central Universities under Grant No. 3103006 and the Foundation of the National Laboratory of Pattern Recognition and funded by the Key Laboratory of Geo-informatics of the State Bureau of Surveying and Mapping.

Downloaded by [Wuhan University] at 19:10 07 February 2015

References

Bagan, H., Wang, Q., Watanabe, M., Yang, Y. and Ma, J., 2005, Land cover classification from MODIS EVI times-series data using SOM neural network. *International Journal of Remote Sensing*, **26**, pp. 4999–5012.

Bandyopadhyay, S., Maulik, U. and Mukhopadhyay, A., 2007, Multiobjective genetic clustering for pixel classification in remote sensing imagery. *IEEE Transactions on Geoscience and Remote Sensing*, **45**, pp. 1506–1511.

Campbell, J.B., 2000, *Introduction to Remote Sensing* (London: Taylor & Francis).

Campelo, F., Guimaraes, F.G., Igarashi, H., Ramirez, J.A. and Noguchi, S., 2006, A modified immune network algorithm for multimodal electromagnetic problems. *IEEE Transactions on Magnetics*, **42**, pp. 1111–1114.

Coelho, G.P. and Von Zuben, F.J., 2006, omni-aiNet: an immune-inspired approach for omni optimization. In *Proceedings of ICARIS (International Conference on Artificial Immune Systems)*, 4–6 September 2006, Oeiras, Portugal (Heidelberg: Springer-Verlag), pp. 294–308.

Dasgupta, D., 1999, *Artificial Immune Systems and their Applications* (Berlin: Springer-Verlag).

De Castro, L.N. and Timmis, J., 2002a, *Artificial Immune Systems: a New Computational Intelligence Approach* (London: Springer-Verlag).

De Castro, L.N. and Timmis, J., 2002b, Convergence and hierarchy of aiNet: basic ideas and preliminary results. In *Proceedings of ICARIS* (*International Conference on Artificial Immune Systems*), 9–11 September 2002, University of Kent at Canterbury, UK, pp. 231–240.

De Castro, L.N. and Timmis, J., 2002c, An artificial immune network for multimodal function optimization. In *Proceedings of the IEEE Congress on Evolutionary Computation (CEC'02)*, May 2002, Hawaii, Vol. 1, pp. 699–674.

De Castro, L.N. and Von Zuben, F.J., 2000, An evolutionary immune network for data clustering. In *Proceedings of the IEEE SBRN (Brazilian Symposium on Artificial Neural Networks)*, 22–25 November 2000, Rio de Janeiro, Brazil, pp. 84–89.

De Castro, L.N. and Von Zuben, F.J., 2001, aiNet: an artificial immune network for data analysis. In *Data Mining: a Heuristic Approach*, H.A. Abbass, R.A. Sarker and C.S. Newton (Eds), pp. 231–259 (Hershey, PA: Idea Group).

De Castro, L.N. and Von Zuben, F.J., 2002, Automatic determination of radial basis function: an immunity-based approach. *International Journal of Neural Systems*, **11**, pp. 523–535.

De Franca, F.O., Von Zuben, F.J. and De Castro, L.N., 2005, An artificial immune network for multimodal function optimization on dynamic environments. In *Proceedings of the 2005 Conference on Genetic and Evolutionary Computation (GECCO'05)*, 25–29 June 2005, Washington, DC (New York: ACM Press), pp. 289–296.

Duda, R.O., Hart, P.E. and Stork, D.G., 2001, *Pattern Classification* (2nd edn) (New York: Wiley).

Galeano, J., Veloza, A. and González, F., 2005, A comparative analysis of artificial immune network models. In *Proceedings of the 2005 Conference on Genetic and Evolutionary Computation (GECCO'05)*, 25–29 June 2005, Washington, DC (New York: ACM Press), pp. 361–368.

Gomes, L.C.T., De Sousa, J.S., Bezerra, G.B., De Castro, L.N. and Von Zuben, F.J., 2003, Copt-aiNet and the gene ordering problem. *Information Technology Magazine*, **3**, pp. 27–33.

Hall, D. and Ball, G., 1965, ISODATA: a novel method of data analysis and pattern classification, Technical report, Stanford Research Institute, Menlo Park, CA.

Jensen, J.R., 2005, *Introductory Digital Image Processing, a Remote Sensing Perspective* (3rd edn) (Upper Saddle River, NJ: Prentice Hall).

Jerne, N.K., 1973, The immune system. *Scientific American*, **229**, pp. 51–60.

Jerne, N.K., 1974, Towards a network theory of the immune system. *Annual Immunology*, **125c**, pp. 51–60.

Katsavounidis, I., 1994, A new initialization technique for generalized Lloyd iteration. *IEEE Signal Processing Letters*, **1**, pp. 144–146.

Kruse, F.A., Lefkoff, A.B., Boardman, J.B., Heidebrecht, K.B., Shapiro, A.T., Barloon, P.J. and Goetz, A.F.H., 1993, The spectral image processing systems (SIPS) – interactive visualization and analysis of imaging spectrometer data. *Remote Sensing of Environment*, **44**, pp. 145–163.

Liu, L. and Xu, W., 2006, UOFC-AINet: a fuzzy immune network for unsupervised optimal clustering. In *International Conference on Computational Intelligence for Modelling, Control and Automation and International Conference on Intelligent Agents, Web Technologies and Internet Commerce*, 28 November–1 December 2006, Sydney, Australia (Pisctaway, NJ: IEEE Computer Society), pp. 196–196.

Pal, M., 2008, Artificial immune-based supervised classifier for land-cover classification. *International Journal of Remote Sensing*, **29**, pp. 2273–2291.

Pal, N.P. and Bezdek, J.C., 1995, On cluster validity for the fuzzy c-means model. *IEEE Transactions on Fuzzy Systems*, **3**, pp. 370–379.

Pasti, R. and De Castro, L.N., 2006, An immune and a gradient-based method to train multi-layer perceptron neural networks. In *Proceeding of the 2006 IEEE International Joint Conference on Neural Networks*, 6–21 July 2006, Vancouver, BC, Canada, pp. 2075–2082.

Perelson, A.S., 1989, Immune network theory. *Immunological Review*, **110**, pp. 5–36.

Downloaded by [Wuhan University] at 19:10 07 February 2015

Storvik, G., Fjortoft, R. and Solberg, A.H.S., 2005, A bayesian approach to classification of multiresolution remote sensing data. *IEEE Transactions on Geoscience and Remote Sensing*, **43**, pp. 539–547.

Tadjudin, S. and Landgrebe, D.A., 2000, Robust parameter estimation for mixture model. *IEEE Transactions on Geoscience and Remote Sensing*, **38**, pp. 439–435.

Timmis, J. and Edmonds, C., 2004, A comment on opt-AiNet: an immune network algorithm for optimisation. In *Proceedings of the 2004 Conference on Genetic and Evolutionary Computation (GECCO'04)*, 24–26 June 2004, Seattle, WA, D. Kalyanmoy *et al*. (Eds), Lecture Notes in Computer Science 3102 (Heidelberg: Springer-Verlag), pp. 308–317.

Xie, X.L. and Beni, G., 1991, A validity measure for fuzzy clustering. *IEEE Transactions on Pattern Analysis and Machine Intelligence*, **13**, pp. 841–847.

Yamazaki, T. and Gingras, D., 1999, Unsupervised multispectral image classification using MRF models and VQ method. *IEEE Transactions on Geoscience and Remote Sensing*, **37**, pp. 1173–1176.

Zhang, L., Zhong, Y., Huang, B. and Li, P., 2007, A resouce limited artificial immune algorithm for supervised classification of multi/hyper-spectral remote sensing image. *Internal Journal of Remote Sensing*, **28**, pp. 1665–1686.

Zhao, X., Gao, X.S. and Hu, Z.C., 2007, Evolutionary programming based on non-uniform mutation. *Applied Mathematics and Computation*, **192**, pp. 1–11.

Zhong, Y., Zhang, L., Gong, J. and Li, P., 2007, A supervised artificial immune classifier for remote sensing imagery. *IEEE Transactions on Geoscience and Remote Sensing*, **45**, pp. 3957–3966.

Zhong, Y., Zhang, L., Huang, B. and Li, P., 2006, An unsupervised artificial immune classifier for multi/hyperspectral remote sensing imagery. *IEEE Transactions on Geoscience and Remote Sensing*, **44**, pp. 420–431.

Downloaded by [Wuhan University] at 19:10 07 February 2015